The International Journal of Advanced Manufacturing Technology (2019) 103:1925–1934
https://doi.org/10.1007/s00170-019-03663-9

ORIGINAL ARTICLE

Tool orientation optimization considering cutter deflection error caused by cutting force for multi-axis sculptured surface milling

Xianyin Duan [1,2] · Fangyu Peng [2] · Kunpeng Zhu [3] · Guozhang Jiang [4]

Received: 16 October 2018 / Accepted: 27 March 2019 / Published online: 13 April 2019

Abstract
Multi-axis milling (especially five-axis) is in the ascendant for high precision manufacturing of a product with a sculptured surface such as ship propeller, owing to its multi-axis linkage and resulting outstanding superiorities. Needs of a faster-improving manufacturing level of sculptured surface milling are derived by higher performance requirement of complicated equipment, which makes the planning of tool orientations more significant and challenging. This paper builds a tool orientation optimization model with inclusion of the influence of deflection error caused by cutting force to achieve better machining precision controlling in five-axis sculptured surface milling. The basic idea of the optimization method is described firstly, followed by the prediction of cutter deflection error. Then determining processes of the related subset to restrain the tool orientations are developed. Lastly, comparative experiments are designed and performed through milling a propeller rotor possessing numerous blades in a five-axis machining center. By comparison with several other tool orientation methods, the average values and volatility of deflection error are both suppressed better utilizing the optimization modeling. The experiment results reflect that it is insufficient to consider single geometric constraint or kinematic constraint, and greater attention should be paid to the role of cutter deflection caused by cutting force in planning the tool orientations.

Keywords Tool orientation · Cutting force · Cutter deflection · Multi-axis milling

1 Introduction

Multi-axis synchronous milling, bringing two or more rotation axes for traditional milling, is in the ascendant owing to its multiple advantages, especially in the milling of a sculptured surface. Through controlling two rotational degrees of freedom, the NC system can allow the tool orientation to be in any direction. Then avoiding interference becomes easier in the machining of parts with complex structural features or confined space. The machining efficiency can also be improved by optimizing engagement curve between the workpiece and the cutter. Meanwhile, there are some challenges going along with multi-axis milling. Taking the example of the shipbuilding industry, the core parts, such as the screw propeller, are designed with many difficult-to-machine features such as narrow reachable workspace of tool orientations and weak stiffness of the cutting tool and workpiece (Fig. 1), as the needs of machine performance become increasingly higher.

The flexibility of the manufacturing process system is amplified by more driving and moving components on account of more freedom of movement. Furthermore, multitudinous difficult-to-machine features of the sculptured surface part

✉ Xianyin Duan
duanxianyin@163.com

Fangyu Peng
pengfy@hust.edu.cn

Kunpeng Zhu
zhukp@iamt.ac.cn

Guozhang Jiang
whjgz@wust.edu.cn

[1] Hubei Key Laboratory of Mechanical Transmission and Manufacturing Engineering, Wuhan University of Science and Technology, Wuhan, China

[2] State Key Laboratory of Digital Manufacturing Equipment and Technology, Huazhong University of Science and Technology, Wuhan, China

[3] Institute of Advanced Manufacturing Technology, Hefei Institutes of Physical Science, Chinese Academy of Science, Changzhou, China

[4] Key Laboratory of Metallurgical Equipment and Control Technology, Ministry of Education, Wuhan University of Science and Technology, Wuhan, China

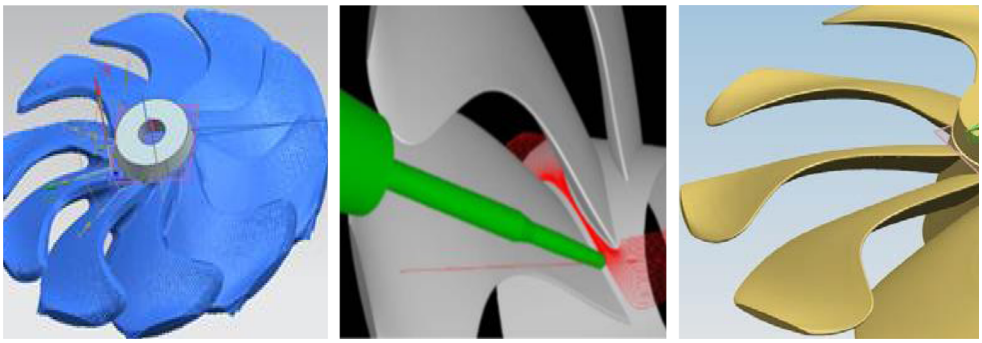

(a) Overlap region of the blade is higher than 16%

(b) length-width ratio of the passage is higher than 13:1

(c) overhanging length-thick ratio of the blade is higher than 15:1

Fig. 1 A type of propeller with many difficult-to-machine features. **a** Overlap region of the blade is higher than 16%. **b** Length-width ratio of the passage is higher than 13:1. **c** Overhanging length-thick ratio of the blade is higher than 15:1

make the slenderness ratio of the cutter get very large, which weakens the stiffness of the cutter. Complicated features of the part also can bring about greater material removal ratio usually, which enlarges the thickness and width of the chip. As a result, the cutting forces get higher. Under the conditions of greater cutting force and lower rigidity of the processing system and the cutting tool, the influence of cutter deflection caused by cutting force on the machining precision becomes non-ignorable. Therefore, this work studies the control of cutter deflection error through optimizing the tool orientations for five-axis milling of a sculptured surface part.

Many efforts are taken for the tool orientation generation in the multi-axis machining. Fan et al. [1] proposed the cutter posture optimization method which could enlarge the effective cutting width in the flat-bottomed machining. Kim et al. [2] proposed the method to obtain an optimal tool path which could avoid various interferences effectively for multi-axis milling. Li et al. [3] designed a cutter posture planning method which was based on the cutting tool partition and could remove typical over cutting phenomena for multi-axis milling. Those signs of progress are from a geometric perspective, aiming to avoid collision between the tool and parts of the machine tool, machined part, or the fixtures.

There are also many advances in the research of contact relationship of the two effective cutting curves from the cutter swept surface and the designed part. Zhu et al. [4] studied the cutter posture determination for the five-axis milling, whose aim was to maximize the mean width of the cutting line. Chen et al. [5] presented the approach of planning tool orientation that was based on the MPECM method in which the optimizing goal was replaced with multipoint tool orientation. Wu et al. [6] presented the method to adjust the cutting line width for five-axis machining and avoid needless overlay of adjoining paths. Gan et al. [7] presented the approach based on mechanical equilibrium for obtaining the optimized tool orientation which could enlarge the cutting line width. Those achievements contribute to the improvement of machining efficiency. Lots of achievements have also been obtained in the aspect of smoothness [8–11]. In those researches, kinematic methods are proposed and realized.

Further, many scholars explore the influence relations of the tool orientations on the cutting load, surface finish, etc. Geng et al. [12] studied by simulation to determine the cutter postures which took the cutting load into account, but the tool–workpiece engagement was confined to ball-end component. Sung et al. [13] built the theoretical model to obtain the surface roughness using parameters such as feed speed and the tool geometric parameters in the lathe. Campatelli et al. [14] presented a method for bringing down the influence of outside interference through optimizing the location and posture of the workpiece in the NC miller. There are also many studies having been performed from the point of the experiment for tool orientation planning [15–17].

From the above analysis, the methods to plan the tool orientations methods have been extensively studied, but informed studies are mainly limited to the geometric field of processing systems such as the fixture, the milled workpiece, and the cutting tool; kinematical level of the processing equipment such as the machine tool and the industrial robot; and so forth. Lesser explorative research including some non-geometric and non-kinematical objects is conducted, such as joining the role of the cutting force or stiffness. However, little research is known about taking the influence of tool orientation on deflection error caused by cutting force into consideration for multi-axis machining of a sculptured surface part.

With fast advances of transportation industry such as shipbuilding, key components with a sculptured surface are meeting a broader range of applications. Needs of higher performance parameters of the engineering equipment put needs of higher milling precision of multi-axis machining forward. In practice, different tool orientations could result in different cutter deflection error caused by cutting force in multi-axis machining, which is also confirmed via our tests. To meet these needs and challenges, we aim at optimizing the tool orientations at a certain location and contact trajectory in multi-axis milling of sculptured surface part, for realizing better deflection controlling under the premises of avoiding multiple interferences and collisions and overlarge vectoring deflection angle.

Based on preliminary researches on the error controlling, estimation of cutting force, and cutter deflection [18–22], the influence of cutter deflection on the control of milling error is investigated and used in the tool orientation optimization. The rest of this work is structured as follows. In Section 2, an optimization model considering deflection error is built and implemented. Experiments of machining representative part are designed and conducted to compare the error values between the proposed method and existing common methods in Section 3. We make several conclusions in Section 3.2.

2 Optimization modeling and implementation

2.1 Basic idea of the optimization method

Tool orientation, the axis of the cutter in the local coordinate system, could be described by the vector (v) or the attitude angles of the axis. The two descriptions could be deduced by each other as

$$\mathbf{v} = \mathbf{x}\sin\alpha\cos\beta + \mathbf{y}\sin\alpha\sin\beta + \mathbf{z}\cos\alpha \tag{1}$$

where, ($\boldsymbol{x}$, $\boldsymbol{y}$, $\boldsymbol{z}$) denote the coordinate axes of local coordinate system; (α, β) are two attitude angles of the axis, which have two definitions as shown in Fig. 2. Researchers usually adopt the definitions of Fig. 2a, in which α is the angle between $\boldsymbol{z}$ and $\boldsymbol{v}$ and β is the angle between $\boldsymbol{O_CA}$ and $\boldsymbol{O_CB}$. The definitions according to Fig. 2b could be seen in much CAM software in which α is the angle between $\boldsymbol{z}$ and $\boldsymbol{v}'$ and β is the angle between $\boldsymbol{z}$ and $\boldsymbol{v}''$. The first definitions are used in this paper, which could be easily converted to the second definitions by derivation of equation if needed.

The set of every tool orientation in idea state is spherical surface which could be mapped to a disc, as shown in Fig. 3.

As shown in Fig. 4, the leftmost circle S_G denotes set of all the tool orientations. V_G and V_d are both subset of S_G, which denotes set of tool orientations from a different perspective. V_G contains all the tool orientations meeting in the requirement of avoiding multiform interferences. V_d is a subset of tool orientations that could maintain the cutter deflection under a specific value. Tool orientations that could satisfy simultaneously the above two requirements form a subset V_{Gd}. In V_{Gd}, calculation and search could be carried out to look for the tool orientation $v_{e,\min}$ leading to minimal deflection error. Then, to increase the smoothness of the motion axes, the neighborhood of the $v_{e,\min}$ is generated as feasible space $V_{e,\text{smooth}}$. Then the smoothing process is conducted within $V_{e,\text{smooth}}$ for the optimal tool orientation $v_{e,\ \text{opt}}$, which synthetically considers avoiding the interference, kinematic smoothing, and the deflection error.

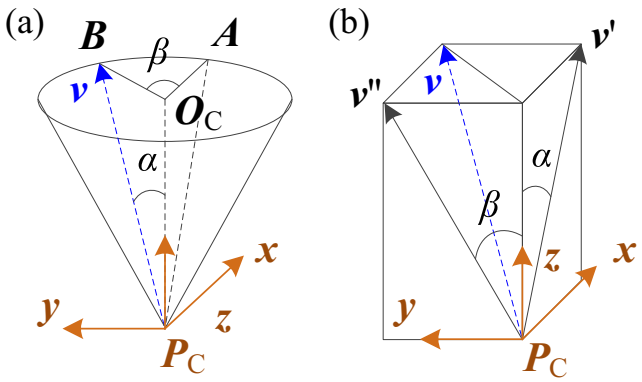

Fig. 2 **a**–**b** Two definitions of the lead angle and the tilt angle

2.2 Prediction of cutter deflection error

The tool–workpiece geometric transform relationship is the basis for the prediction of cutter deflection error. As shown in Fig. 5, (x_T, y_T, z_T) and ($\boldsymbol{x}$, $\boldsymbol{y}$, $\boldsymbol{z}$) are respectively the coordinate axes in coordinate system of tool ($\boldsymbol{v}_T$) and coordinate axes in local coordinate system whose original points are respectively $\boldsymbol{P}_T$ and $\boldsymbol{P}_W$.

The tool–workpiece geometric transform relationship could be developed as

$$\begin{cases} \mathbf{P}_T = \mathbf{P}_W + r\cdot(\mathbf{z}-\mathbf{z}_T)-(R-r)\cdot\mathbf{x}_T, \\ \mathbf{v}_T = \left(\dfrac{\mathbf{v}_W \times (\mathbf{P}_{T,i+1}-\mathbf{P}_{L,i}) \times \mathbf{v}_W}{\|\mathbf{v}_W \times (\mathbf{P}_{T,i+1}-\mathbf{P}_{L,i}) \times \mathbf{v}_W\|}, \dfrac{\mathbf{v}_W \times (\mathbf{P}_{T,i+1}-\mathbf{P}_{T,i})}{\|\mathbf{v}_W \times (\mathbf{P}_{T,i+1}-\mathbf{P}_{T,i})\|}, \dfrac{\mathbf{v}_W}{\|\mathbf{v}_W\|} \right). \end{cases} \tag{2}$$

where R and r are respectively the radius of the cutter and the cutter arc; $\boldsymbol{v}_w$ is the tool orientation in the coordinate system of the workpiece.

Then the radial immersion angle φ_{jc} at the contact-moment when the elemental chip $\boldsymbol{P}_{ce}$ overlaps with the cutter contact point $\boldsymbol{P}_{cc}$ could be obtained as

$$\varphi_{jc} = \begin{cases} \arctan\left(\dfrac{{}^{L}P_{cy}}{{}^{L}P_{cx}}\right) + (j-1)\varphi_p - 2z\cdot\tan\left(\arctan\left(\tan\beta_t\cdot\sqrt{r^2-(r-z)^2}/r\right)\right)/D, & z < r, \\ \arctan\left(\dfrac{{}^{L}P_{cy}}{{}^{L}P_{cx}}\right) + (j-1)\varphi_p - 2z\cdot\tan\beta_t/D, & z \geq r, \end{cases} \tag{3}$$

where ${}^{L}P_{cx}$ and ${}^{L}P_{cy}$ are x-coordinate and y-coordinate of cutter contact point under a coordinate system of cutter location point; φ_p and β_t are respectively pitch angle and nominal spiral angle of a cutting tool.

From Eq. (3) and theoretical models of cutting force and synthetic flexibility at the end of machining system proposed in [21], the three-dimensional cutter deflection at the contact-moment $\boldsymbol{d}_{tc}$ could be deduced as

$$\mathbf{d}_{tc} = \mathbf{S}_C\,\mathbf{f}_{jc}, \tag{4}$$

where $\boldsymbol{f}_{jc}$ is instantaneous cutting force when the cutter rotation angle is φ_{jc}; $\boldsymbol{S}_C$ is synthetic flexibility at the end of machining system.

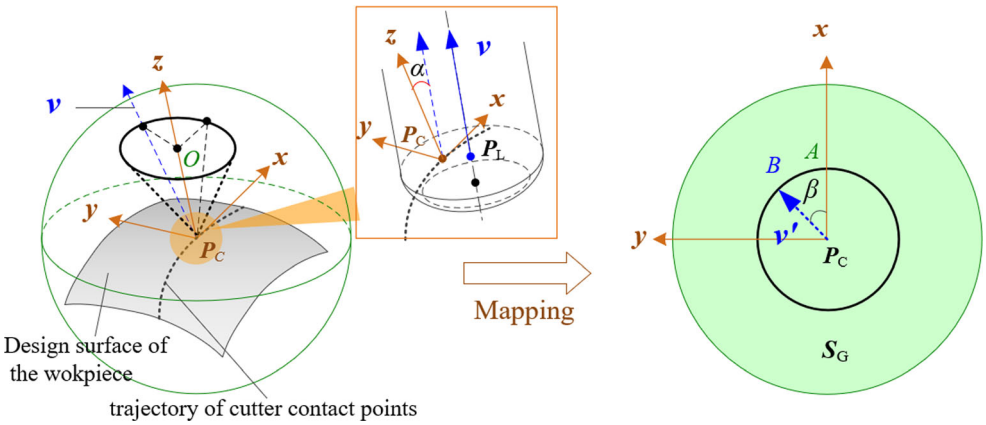

Fig. 3 Tool orientations mapping as a disc

Equation (4) reveals the influence relation of orientation on deflection caused by cutting force. To further reflect the connection between orientation and the machining precision, the surface error $\boldsymbol{e}_{cz}$ is mapped from the deflection and built as

$$e_{cz}(\alpha,\beta) = d_{tcz}\cos\alpha\cos\beta - d_{tcx}\sin\alpha + d_{tcy}\cos\alpha\sin\beta. \tag{5}$$

2.3 Determining of the related subset

(1) Determining of V_G

As mentioned above, V_G contains the tool orientations meeting in the requirement of avoiding multiform interferences. The intersection of those interferences generates the result of V_G which is shown in the following equation.

$$V_G = V_{Ts} \cap V_\kappa \cap V_{Tb} \cap V_M. \tag{6}$$

where V_{Ts} generates result avoiding the interference between the shank surface and the machined part; V_k is used to avoid interference because the curvature of the effective cutting curve is less than the maximum curvature at the cutter contact point; V_{Tb} needs to avoid interference between the cutting edge swept surface and design surface of the workpiece; the function of V_M is to avoid interference between the tool swept surface and the machine tool parts and fixtures. They could be determined by

$$\begin{cases} V_{Ts}(\mathbf{P}_{i,j}) = \{\mathbf{v} | d_{\min}(S_{Ts}(\mathbf{P}_{i,j},\mathbf{v}), S_W) > \delta_{Ts}\} \\ V_\kappa(\mathbf{P}_{i,j}) = \{\mathbf{v} | \kappa_T(\mathbf{P}_{i,j},\mathbf{v}) > \kappa_{\max}(\mathbf{P}_{i,j})\} \\ V_{Tb}(\mathbf{P}_{i,j}) = \{\mathbf{v} | d_{\min}(S_{Tb}(\mathbf{P}_{i,j},\mathbf{v}), S_W) > \delta_{Tb}\} \\ V_M(\mathbf{P}_{i,j}) = \{\mathbf{v} | d_{\min}(S_{Ts}(\mathbf{P}_{i,j},\mathbf{v}), S_M) > \delta_M\} \end{cases} \tag{7}$$

(2) Determining of V_d

To protect the cutter from damage, the cutter deflection needs to be maintained under a specific value. V_d is designed to play the role, which is determined by

$$d(\alpha,\beta) < \delta d. \tag{8}$$

where d denotes the synthetic deflection of three coordinate axis directions, whose calculation referenced the method from [21]; δd denotes the threshold value that is related to a number of factors such as the grade of precision; size and material of the cutting tool; and size and material of the workpiece.

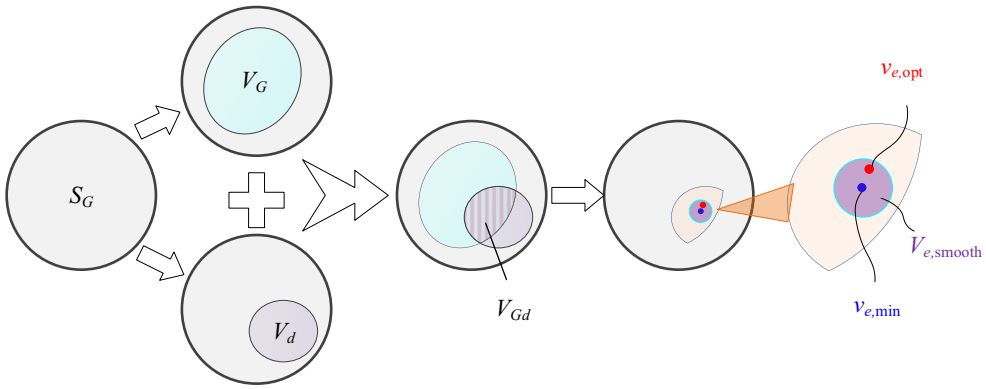

Fig. 4 Tool orientation planning method

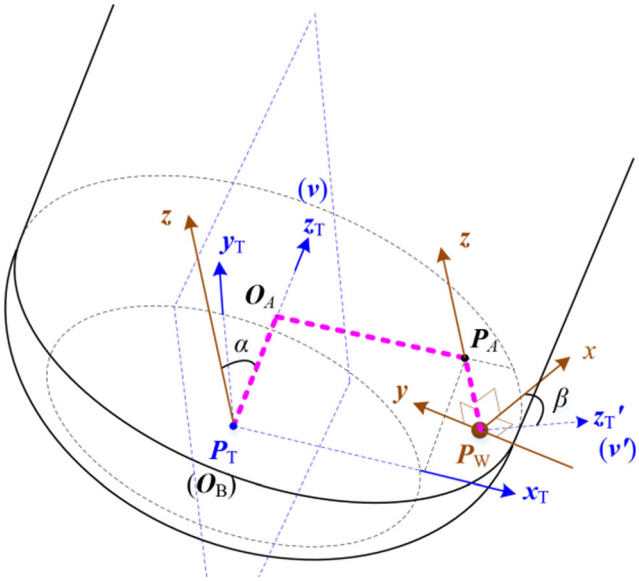

Fig. 5 The tool–workpiece geometric transform relationship

(3) Smoothness operation

Firstly, the movements of the machine tool are limited to the permissible scope, which is realized by

$$\mathbf{M}_{i,j} \in \left[\mathbf{M}_{i,j,\min}, \mathbf{M}_{i,j,\max}\right]. \tag{9}$$

where the component of $\boldsymbol{M}$ is each machine tool axis.

On the basis, the tool orientation variation follows

$${}^{\mathrm{W}}\Delta\mathbf{v} = \sqrt{\sum_{j=1}^{N_P}\sum_{i=1}^{N_L}\left(\left(\arccos\left(\mathbf{v}_{i,j},\mathbf{v}_{i+1,j}\right)\right)^2 + \left(\arccos\left(\mathbf{v}_{i,j},\mathbf{v}_{i,j+1}\right)\right)^2\right)} < \delta_{\mathrm{v}}, \tag{10}$$

where i is the sequence of cutter location points at the same tool path, j is the sequence of tool paths, N_L is the sequence number of the cutter location points at the same tool path, and N_P is the sequence number of the tool paths.

(4) Determining of the feasible tool orientation set

The determination flow of set of feasible tool orientation is shown in Fig. 6. The initial conditions (the discrete points $\boldsymbol{P}_{i,j}$ from the design surface S_D of the workpiece, the geometric parameters of the cutter and the processing equipment, the kinematic parameters of the processing equipment, etc.) are set and input for following calculations. The set of interference-free tool orientations are then calculated by Eq. (6). Three constraint conditions shown in Fig. 6 constrain the tool orientations in a feasible space.

2.4 Determining the optimal tool orientation

The mapped result of the cutter deflection could directly reflect the milling precision. So, the deflection error is adopted as the optimizing goal and shown as

$$\min\left(d_{tcz}\cos\alpha\cos\beta - d_{tcx}\sin\alpha + d_{tcy}\cos\alpha\sin\beta\right) \tag{11}$$

Based on the above steps, the lead angles and tilt angles are searched for minimal deflection error $e_{cz,\min}$. Quick search algorithm, namely the genetic algorithm, is applied to speed the searching process for $v_{e,\min}$ that leading to minimal deflection error. The optimal tool orientation $v_{e,\,\mathrm{opt}}$, is obtained in the neighborhood space of $v_{e,\min}$, after the smoothing operation.

3 Experimental setup and verification

3.1 Experimental setup

In the experiment setup, a rough machined proportionally reduced ten-blade propeller rotor is chosen to verify the developed approach. The workpiece material is ZCuAl8Mn13Fe3Ni2, the high manganic aluminum bronze as shown in Fig. 7, which shows excellent performances (dense alloy microstructure, strong corrosion resistance, and high corrosion fatigue strength) in the seawater, and is used in the fields of navigation for manufacturing marine blade rotor. So this material is chosen as the workpiece material in the experiment. Two location holes are set at the fixture to determine the rotation angle of the propeller rotor. The machining process is arranged as semi-finishing machining at partial regions of the propeller blades whose surface features and allowances are nearly the same.

Figure 8 shows the milling experiment site including the processing equipment, the cutting tool, the processing workpiece, etc. The types or values of the main parameters used in the milling experiments are listed in Table 1.

The experimental platform is arranged on the five-axis machining center (Mikron UCP 800 Duro). The machining parameters and experimental conditions of the processing system and the data acquisition instrument are shown in Table 1.

The six groups of experiments are designed and listed in Table 2. Machining process corresponding to each group is carried out on a predetermined blade respectively. The trajectory of the cutter contact points in each group is the same with varying tool orientations. The first method is known as vertical milling, in which all the tool axis vectors are (0, 0, 1). That milling method is widely used in three-axis machining and five-axis machining of simple surface parts. The method used in the second group makes the tool axis perpendicular to the tangential plane at each cutter contact point. That method is a commonly chosen option in the business CAM software. The tool attitude angles in the third method remain as (10°, 0). That

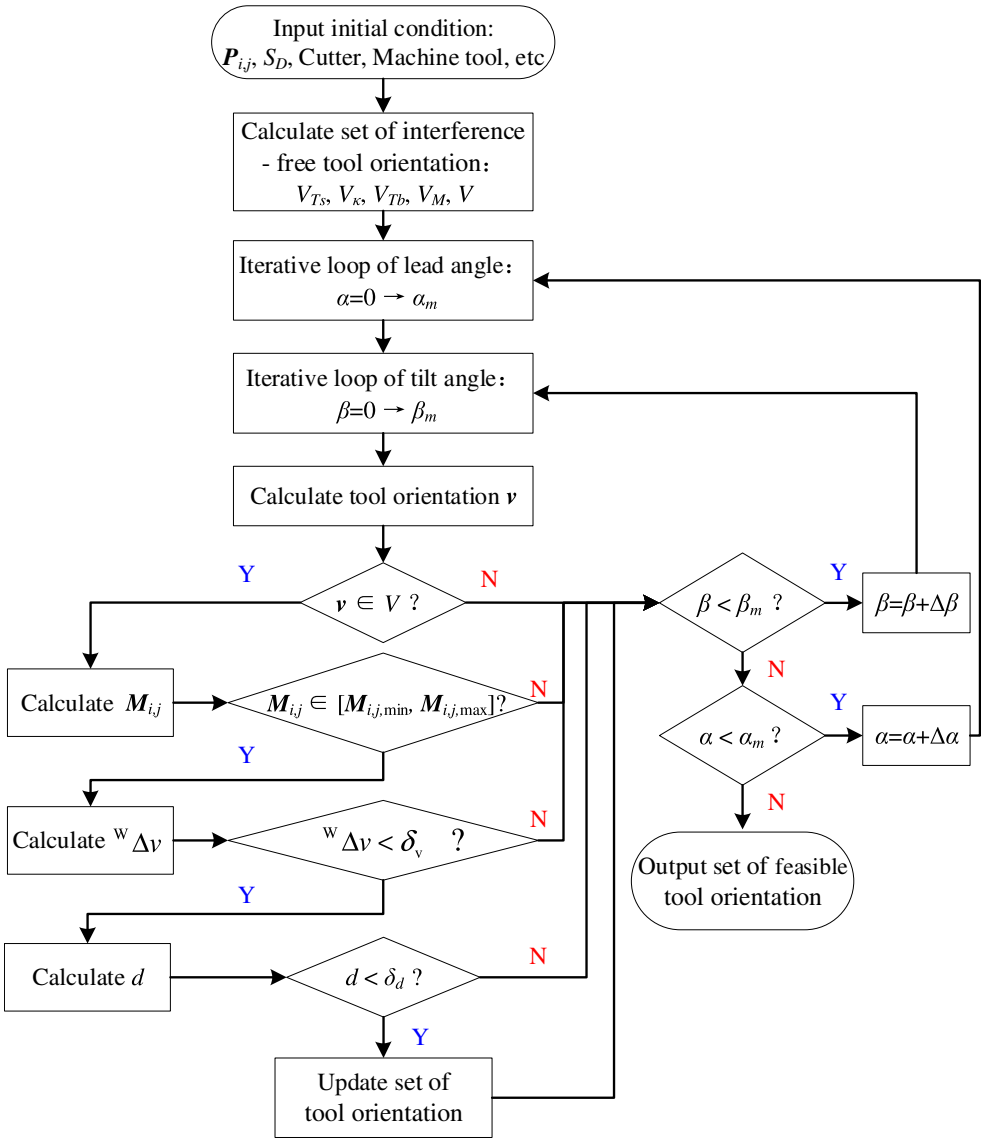

Fig. 6 Determination of feasible tool orientation set

Fig. 7 Experiment setup of the workpiece

is obtained through a survey in a propeller processing enterprise. In the fourth method, the tool axes are based on normal vectors at each point and then smoothed to avoid oversize rotation angles of the adjacent tool axes, to show the effect of only considering smoothness. Group 5 uses the tool orientations generated by our optimization method. Optimized tool attitude angles are applied in the last group to demonstrate the proposed method.

Machining parameters and conditions set in the milling experiments are shown in Table 3. In the table, L_o denotes the overhanging length of the cutter. n denotes the rotating speed of the spindle. F denoted the feed speed. a_p denotes the machining allowance.

As marked on the workpiece surfaces shown in Fig. 7, all the feed directions are set along the parametric curves of the workpiece design surfaces, from the blade tip to the blade root.

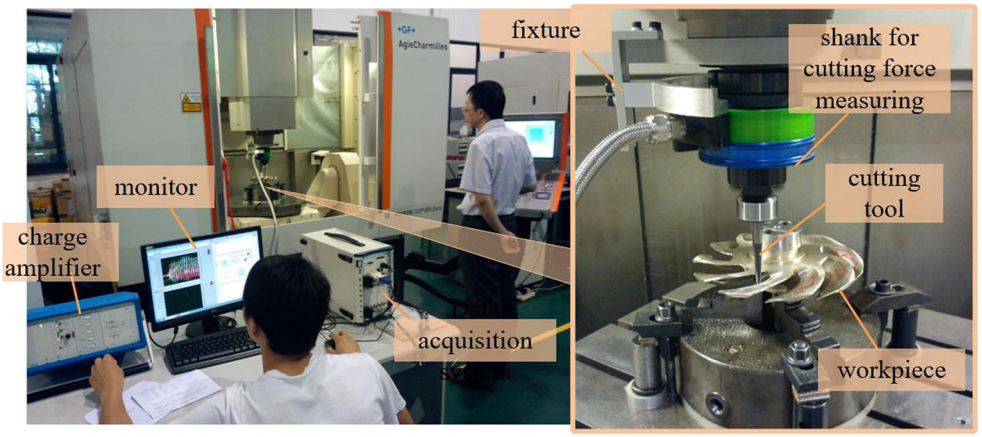

Fig. 8 Experiment setup of the machining process

The cross feed direction is all set along the helix direction of the workpiece design surfaces. Though isoparametric tool-path planning, 80 semi-finish machining tool paths are generated at machining region of each blade. Ten tool paths are grouped as one measurement period.

After the machining process, the workpiece remains in situ and the cutter is changed to a position measuring probe. Coordinates of 16 positions from the machining region, as shown in Fig. 9a, are designed as the measured points. The measuring probe orientations at all the positions remain along the normal vector at the points of the semi-finish machined surface. Radius compensation of the probe is conducted by the measuring system to generate the coordinate data. Then the machining error values could be calculated from the ideal coordinates and measured coordinates.

3.2 Result and discussion

The measured five groups of machining errors of the blades are exhibited in Fig. 10, each of which contains 4 × 4 values from corresponding measured points. From Fig. 10, there is no negative value, which means that no undercutting occurs during the milling process. The major reason for the undercutting appearance is the cutter relieving, which are caused by cutting forces and result in small amounts of allowances. The cutter relieving would not make the machined parts be waste products but probably generate unaccepted products needing additional post-processing when the resulted errors become excessive.

As shown in Fig. 10, regular peaks and valleys appear from the error curves, which are directly related to the locations of chosen measuring points. As to all the measured surfaces, the measuring processes are the same, such as the chosen regions measured from the surfaces (reflecting surface features), the measuring paths (along helix curves of the propeller surface), and the coordinates of measured points under respective coordinate system of propeller blade. Then they have similar normal vectors, stiffness characteristics, and cutter–workpiece engagements, which cause similar cutting forces and cutter deflections. Therefore, measured points with the same sequence number on respective propeller blade have similar features of error values.

From Fig. 10, the third method performs the worst in the error controling, especially at Point No. 2 and Point No. 11 being close to 0.05 mm, and highest volatility. When the α is a certain unchanged angle and the β remains as 0, the cutter will only change depending on the normal vector, and do not care any cutter–workpiece engagement, configuration of the machine tool transmission axes, or relationship among coordinate systems of the processing system (being not concerned with V_d or $v_{e,min}$ in Fig. 4). Then large cutting force occurs, so does cutter deflection and machining error.

Table 1 Parameters in the milling experiments

Main parameters	Types or values
Processing equipment	Mikron UCP 800 Duro
Workpiece material	ZCuAl8Mn13Fe3Ni2
Cutting force measuring instrument	Kistler 9123
Cutting force collection instrument	NI PXIe - 1082
Tool type	Conical ball-end mill with 4-flute
Length of the cutter (mm)	100
Length of the flute (mm)	40
Diameter of the cutter shank (mm)	10
Position measuring probe	Renishaw OMP40
Diameter of the ruby probe (mm)	6

Table 2 Design of tool orientations in each group

Groups	Design of tool orientations
1	Vertical directions
2	Normal directions
3	Lead angles: 10°, tilt angles: 0
4	Smoothed tool orientations based on normal directions
5	Proposed method of this paper

Table 3 Parameters and conditions of the milling experiments

Machining conditions	Values
L_o (mm)	75
n (rev/min)	4000
F (mm/min)	1000
a_p (mm)	0.4
Cooling condition	No cutting fluid

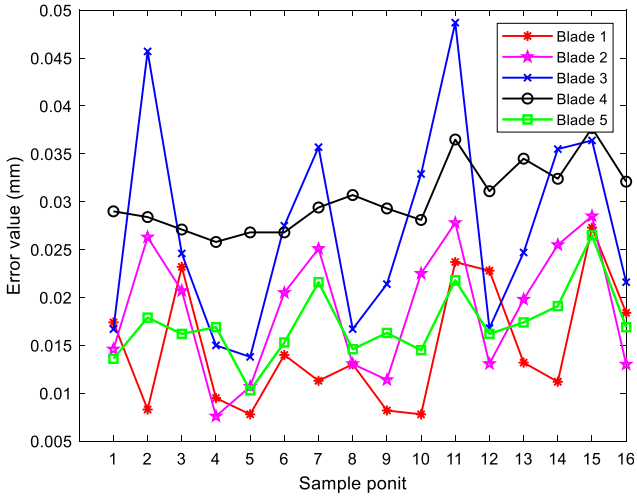

Fig. 10 Comparison of cutter deflection errors

There are rather close variation trends between blade 2 and blade 3, and amplitudes of error values of blade 2 are all smaller than corresponding points of blade 3. Nearly 1/3 points of blade 3 have large errors more than 0.025 mm which is the largest except blade 3 and blade 4. The amplitude of value of blade 3 usually reaches about 0.02 mm which is only second to those of blade 3, from Figs. 10 and 11. The reason is without considering contact geometry between the cutter and the workpiece, stiffness characteristic of the kinematic chain, and the error mapping relationship, similar to that of blade 3. The amplitude reductions may reflect that tool orientations along the normal vectors have better effects than simply setting a stationary tilt angle. Tool posture angle setting without constraints will probably deteriorate the cutting conditions, especially for a sculptured surface workpiece such as propeller rotor blade.

The volatility of results applying the fourth method is the lowest, in which the largest amplitude is 0.012 mm (Figs. 10 and 11). That has a correlation with the role played by the smoothness operation which makes tool orientations of adjacent points take the kinematic changes into account and control them through setting constraint condition. However, the average values reach up to 0.03 mm which is the largest. That reflects the contradiction between superior smoothness and better error controlling because the smoothing process could deteriorate overall contact situations for reducing kinematic changes.

The average value applying the first method is roughly comparable to that applying the fifth method. The two methods also both show better error controlling than other methods. In the first method, the tool axis remains vertical, and the workbench remains horizontal. The machine tool works with only three degrees of freedom, so it can provide better stiffness characteristic without the need to work under abnormal configuration or postures. However, the method known as vertical milling could only provide incapacious reachable workspace of tool orientations and could not use as machining of surfaces possessing complex features such as overlapping region of the workpiece in this experiment. In other words, the area of V_G (in Fig. 4) of this method is quite small and most likely inexistent under some machining conditions.

From the perspective of volatility, the values applying the first method undulate more largely than applying the fifth method from Fig. 10. The max difference of the first method is also larger than that of the fifth method, which also reveals the function of smoothness operation. Overall, tool orientations in blade 5 are reachable certainly because they are inside the subset V_G (in Fig. 4). They could also better protect the cutter though restricting the value of cutter deflection inside the subset V_d (in Fig. 4). From the model of cutter deflection, its restraint is actually equivalent to optimize the cutting contact relation to constrain the cutting load and the structure

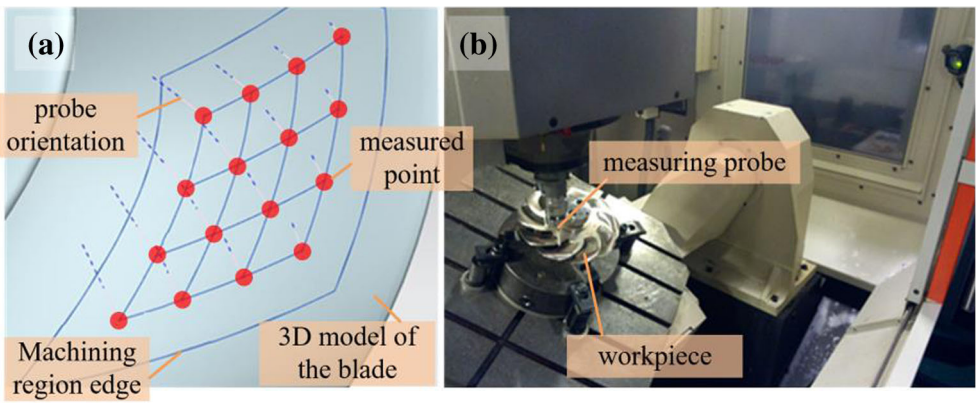

Fig. 9 **a** Measurement scheme and **b** experiment setup of the in situ measuring process

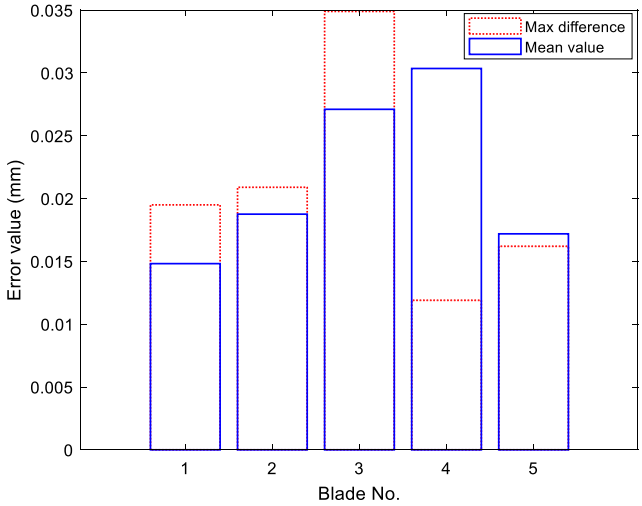

Fig. 11 Comparison of max difference and average value of errors

configuration of the machining system to regulate the stiffness. The optimization of deflection error involves mapping relation from the cutter deflection to surface error, to produce $v_{e,\min}$ (in Fig. 4), which could control the mean error at a lower value. Then the smoothness operation determining the $v_{e,\ opt}$ (in Fig. 4) restrains the volatility and makes the optimized values embody the action of smoothness and error control and balance between them.

4 Conclusions

This study explored the tool orientation optimization to improve the milling precision with the inclusion of the influence of cutter deflection error, and it is validated with propeller rotor milling experiments. In this approach, the deflection error is modeled based on mapping of cutter deflection caused by cutting force along the direction of the surface normal vector. In addition, accessibility and smoothness of the tool axis vector are also included to meet the basic demands. The optimized tool orientation planning model is more balancing for different types of pursuits and could reflect the influence of cutter deflection and resulting error.

In the milling experiments, the workpiece surface has features of the large overlap region, nonlinear lateral slope, and longitudinal slope. Comparison of cutter deflection errors from five varying tool orientation planning methods is derived. From values of 16 points of each blade, deflection error of 81.3% points is below 0.02 mm using the optimized method, which is the highest ratio among all methods. The average value of error applying the optimized method is 0.017 mm, which is only more than the vertical milling method slightly. But the vertical milling method is limited to simple surface machining. The experimental results verify the effectiveness of the optimized method for higher machining precision.

Moreover, in the actual planning process, it is found that massive calculations result in time-consuming planning processes, which brings out the need for further research on model simplification. In future research, stiffness of the workpiece will also be studied to build a closed loop transmission chain containing the machine tool, the cutter, and the workpiece.

Funding information This work was supported by National Natural Science Foundation of China under Grant No. 51605346 and China Postdoctoral Science Foundation under Grant No. 2016M602374.

References

1. Fan J, Ball A (2014) Flat-end cutter orientation on a quadric in five-axis machining. Comput Aided Des 53(5):126–138
2. Kim YJ, Elber G, Bartoň M, Pottmann H (2015) Precise gouging-free tool orientations for 5-axis CNC machining. Comput Aided Des 58(C):220–229
3. Li X, Lee CH, Hu P, Zhang Y, Yang F (2018) Cutter partition-based tool orientation optimization for gouge avoidance in five-axis machining. Int J Adv Manuf Technol 95(5–8):2041–2057
4. Zhu Y, Chen ZT, Ning T, Xu RF (2016) Tool orientation optimization for 3+2 -axis cnc machining of sculptured surface. Comput Aided Des 77(C):60–72
5. Chen ZT, Li SS, Gan ZW, Zhu Y (2017) A highly efficient and convergent optimization method for multipoint tool orientation in five-axis machining. Int J Adv Manuf Technol 93(5–8):2711–2722
6. Wu B, Liang M, Zhang Y, Luo M, Tang K (2018) Optimization of machining strip width using effective cutting shape of flat-end cutter for five-axis free-form surface machining. Int J Adv Manuf Technol 94(5–8):2623–2633
7. Gan ZW, Chen ZT, Zhou M, Yang J, Li SS (2016) Optimal cutter orientation for five-axis machining based on mechanical equilibrium theory. Int J Adv Manuf Technol 84(5–8):989–999
8. Bi QZ, Wang YH, Zhu LM, Ding H (2010) Wholly smoothing cutter orientations for five-axis NC machining based on cutter contact point mesh. Sci China Technol Sci 53:1294–1303
9. Sun YW, Xu JT, Jin CN, Guo DM (2016) Smooth tool path generation for 5-axis machining of triangular mesh surface with nonzero genus. Comput Aided Des 79(C):60–74
10. Sun SX, Sun YW, Xu JT, Lee YS (2018) Iso-planar feed vector-fields-based streamline tool path generation for five-axis compound surface machining with torus-end cutters. ASME J Manuf Sci Eng 140(7):071013
11. Mi Z, Yuan CM, Ma X, Shen LY (2017) Tool orientation optimization for 5-axis machining with c-space method. Int J Adv Manuf Technol 88(5–8):1243–1255
12. Geng L, Liu PL, Liu K (2015) Optimization of cutter posture based on cutting force prediction for five-axis machining with ball-end cutters. Int J Adv Manuf Technol 78(5):1289–1303
13. Sung AN, Ratnam MM, Loh WP (2014) Effect of wedge angle on surface roughness in finish turning: analytical and experimental study. Int J Adv Manuf Technol 74:139–150
14. Campatelli G, Scippa A, Lorenzini L (2014) Workpiece orientation and tooling selection to reduce the environmental impact of milling operations. Procedia Cirp 14(14):575–580
15. Fard MJB, Bordatchev EV (2013) Experimental study of the effect of tool orientation in five-axis micro-milling of brass using ball-end mills. Int J Adv Manuf Technol 67:1079–1089
16. Zahrani EG, Sedghi A (2014) Experimental investigation of precision turning of Monel K-500 under dry conditions. Int J Adv Manuf Technol 73:1265–1272

17. Rodríguez P, Labarga JE (2015) Tool deflection model for micromilling processes. Int J Adv Manuf Technol 76(1–4):199–207
18. Peng FY, Ma JY, Wang W, Duan XY (2013) Total differential methods based universal post processing algorithm considering geometric error for multi-axis NC machine tool. Int J Mach Tools Manuf 70(70):53–62
19. Duan XY, Peng FY, Yan R, Zhu ZR, Li B (2015) Experimental study of the effect of tool orientation on cutter deflection in five-axis filleted end dry milling of ultrahigh-strength steel. Int J Adv Manuf Technol 81(1–4):653–666
20. Zhu ZR, Yan R, Peng FY, Duan XY, Zhou L, Song K (2016) Parametric chip thickness model based cutting forces estimation considering cutter runout of five-axis general end milling. Int J Mach Tools Manuf 101:35–51
21. Duan XY, Peng FY, Yan R, Zhu ZR, Huang K, Li B (2016) Estimation of cutter deflection based on study of cutting force and static flexibility. J Manuf Sci E-T ASME 138(4):041001–041015
22. Duan XY, Peng FY, Zhu KP, Jiang GZ (2019) Cutting edge element modeling-based cutter workpiece engagement determination and cutting force prediction in five-axis milling. Int J Adv Manuf Technol, 3